



## 1. Introduction

The recent advances in nanofabrication methods<sup>1,2</sup> and nanoparticle synthesis<sup>3,4</sup> are leading to the advent of a variety of new nanostructures with unusual physical and chemical properties. Nanostructured free-electron metals are particularly interesting, because they can be resonantly excited by visible light to produce surface plasmon (SP) oscillations.<sup>5</sup> SPs are collective electronic oscillations that lead to surface-bound electromagnetic fields. They are categorized into two classes: propagating surface plasmons or surface plasmons polaritons (SPPs)<sup>3,5</sup> and localized surface plasmons (LSPs).<sup>6</sup> In most cases, both SPP and LSP resonances are present and contribute to the optical characteristics of the nanostructure.<sup>7</sup> The manipulation of the properties of SPs by tailoring the geometric parameters of the nanostructures is the heart of the new field of plasmonics.<sup>5</sup> The plasmonic approach offers an exciting alternative for the manipulation of light in the subwavelength regime.<sup>8</sup> The potential for the development of plasmonic-based technologies is a major driving force in this area, and several promising applications have been suggested. For instance, plasmonic wave-guides could allow the processing of a large amount of information at light speed,<sup>3</sup> superlensing effects offers a new route to beat diffraction limitations in imaging systems,<sup>9</sup> and the inherent subwavelength confinement of the plasmonic field provides a viable alternative for nanolithography.<sup>10</sup> All these examples of application have the potential to bring revolutionary advancements in information processing, device fabrication and imaging technologies. On the other hand, the plasmonics revolution has already arrived to the field of chemical sensing, where SP waves are widely used in important fundamental and practical applications.<sup>2</sup> The capability of SPs to monitor surface-binding events plays a key role in chemical, biochemical, and biomedical research.<sup>11</sup> The market has responded to the demand for reliable plasmonic devices for chemical sensing by providing several options for commercial systems that operate based on the principle of SP excitation.<sup>11</sup>

There are basically three approaches for SP-based chemical sensing. The first relies on the dependence of the surface plasmon resonance (SPR) on the dielectric constant at the metal–dielectric interface. The SPR is then sensitive to the changes in refractive indexes provoked by molecular adsorption, a widely explored property by the bioanalytical community to monitor binding events.<sup>11</sup> The second approach explores the red shift in the LSP absorption of metallic nanoparticles (NPs) due to aggregation to devise colorimetric assays.<sup>12</sup> The classical example for the technological applica-

tion of this approach is the Au nanoparticle-based pregnancy test.<sup>13</sup> Finally, the third approach explores the subwavelength electromagnetic (EM) field localization that accompanies the SP excitations for enhanced spectroscopy, such as surface-enhanced Raman scattering (SERS)<sup>14</sup> and surface-enhanced fluorescence spectroscopy (SEFS).<sup>15</sup> Enhanced spectroscopy methods allow direct molecular identification and single-molecule detection limits.<sup>14</sup>

Plasmonic-based chemical sensing technologies are being successfully applied and commercialized, and the basic research in this area is still attracting much interest. The general objective is to develop new types of plasmonic nanostructures that can improve the analytical figures of merit, such as, detection limits, sensitivity, selectivity, and dynamic range, provided by the commercial systems. Other issues, such as cost, reproducibility, and multiplexing, are also tackled, with the goal of providing the best plasmonic-based platform for chemical analysis. Following these lines, our group has been investigating the interesting phenomenon of light transmission through subwavelength holes (nanoholes) in gold films and found that this class of substrate may provide a few advantages over more common chemical sensing platforms. In this Account, we will discuss our main contributions to this particular field and propose an outlook for the future directions of this approach.

## 2. The Extraordinary Optical Transmission

It is intuitive that the amount of light transmitted through an aperture in an opaque metal sheet should decrease with the hole area. The physics behind this phenomenon has been worked out more than 60 years ago by Bethe,<sup>16</sup> who showed that when the wavelength ( $\lambda$ ) of the transmitted light is larger than the hole diameter ( $d$ ), the transmittance ( $T$ ) is given by  $T \propto (d/\lambda)^4$ . A single hole in an infinitely thin slab was considered in Bethe's formalism.<sup>16</sup> An extension of his approach to real metals<sup>17</sup> and to arrays of holes has been reported.<sup>18</sup> The behavior of nanoholes in real metals with finite thickness was subsequently explored.<sup>19</sup>

The idea that the amount of transmitted light decreases with hole diameter according to Bethe's law remained unchallenged until 1998, when Ebbesen and co-workers realized a seminal experiment on the light transmission through arrays of nanoholes in Ag and Au thin films.<sup>20,21</sup> Their result indicated that the amount of transmitted light at certain wavelengths was much larger than predicted by the classical aperture theory. They also demonstrated that there was more light transmitted than the actual amount that impinged on the

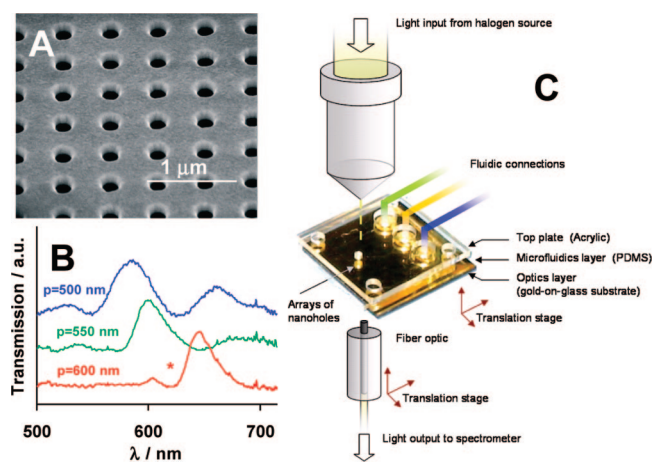


**FIGURE 1.** (A) Scanning electron micrograph (SEM) of an array of nanoholes in a gold film; (B) EOT spectra for three arrays with different periodicities—the asterisk shows the position of the Wood's anomaly for one of the arrays; (C) experimental setup used by our group to measure the EOT effect.<sup>26</sup> The metal film is deposited on a glass slide, and the gold side of the array is exposed to solvents and aqueous solutions delivered by microfluidics.

hole area; that is, the material seemed much more transparent than it should be. This unexpected phenomenon was called extraordinary optical transmission (EOT). The effect was observed for gold and silver films, but its magnitude decreased when different metals were used. Moreover, the peaks of maximum transmission were related to the distance between the nanoholes (periodicity). Considering all these properties, it was suggested that EOT was due to the excitation of surface plasmon resonances by a grating coupling.<sup>20</sup> Although this interpretation has since been challenged,<sup>22</sup> the evidence from several laboratories seem to consolidate the excitation of SP as the main contribution to the EOT effect.<sup>23,24</sup>

An example of an array of nanoholes on Au that supports EOT in the visible range is presented in Figure 1A. The array in Figure 1A was fabricated using focused ion beam (FIB) milling. The EOT effect is illustrated in Figure 1B where the white light transmission spectra through arrays of nanoholes of different periodicities are shown. The spectra in Figure 1B were obtained using a microscope coupled to a miniature spectrometer, as depicted in Figure 1C.<sup>25</sup> Peaks in the white light transmission (Figure 1B) correspond to the wavelengths that match the EOT conditions for each structure. The amount of transmitted light at the peaks far exceeded that expected from the simple aperture theory.<sup>20</sup>

For periodic metallic nanostructures, the phase-matching condition for SPP excitation coincides with the Bragg resonances of the grating. At normal incidence, the wavelength of

SPP resonance ( $\lambda_{\text{SP}}$ ) from an array of nanoholes with square lattice symmetry can be estimated using<sup>20</sup>

$$\lambda_{\text{SP}}(i, j) = \frac{p \sqrt{\frac{\epsilon_d \epsilon_m}{\epsilon_d + \epsilon_m}}}{\sqrt{j^2 + i^2}} \quad (1)$$

where  $p$  is the lattice constant (periodicity) of the array,  $i$  and  $j$  are integers that define the scattering orders of the array,  $\epsilon_d$  and  $\epsilon_m$  are the real part of the dielectric constants of the adjacent medium and the metal, respectively. Equation 1 is for SPs on a smooth metal–dielectric interface, and it does not directly apply for meshes. The EOT phenomenon from metallic meshes and its applications have been recently reviewed elsewhere.<sup>27</sup>

The zero-order (normal incidence) transmission spectra of arrays with different periodicities (Figure 1B) shows EOT slightly red-shifted from that expected from eq 1. Another interesting feature from the EOT spectra shown in Figure 1B is the asymmetry around the transmitted peaks. The minimum in the transmission curves, marked with asterisks in Figure 1B, correspond to a diffraction phenomenon known as Wood's anomaly. A Fano analysis has been suggested to explain the observed red shift of the SP resonance relative to eq 1 and the line-shape asymmetry in the transmissions.<sup>28</sup> The Fano treatment takes into consideration interfering resonant and a nonresonant contributions to the phenomenon. In the specific case of nanohole arrays, the interference between the direct transmission through the nanoholes (incoherent path) and the SP-mediated transmission (coherent path) accounts for the resonance shift and asymmetry observed experimentally in EOT.<sup>28</sup> On the other hand, recent experiments using two stacked micromeshes, which eliminate the direct transmission path, still presented asymmetric transmission peaks.<sup>29</sup>

EOT was also observed for single holes, and contributions from LSPs play a key role in these cases.<sup>19,30</sup> The light transmission depends strongly on the hole shape. For instance, longitudinal and transverse LSP modes can be individually excited in rectangular holes by controlling the electric polarization of the incident light. It has also been found that the cut-off wavelength for the transmission increases as the width of the rectangular holes is reduced, which is another counterintuitive result from nanoholes in metals.<sup>31</sup> The effect of the hole shape on the transmission is also observed from arrays of nanoholes.<sup>32,33</sup> Another interesting property related to EOT from single holes is the “beaming” of the transmitted light,<sup>19</sup> which is a preferential direction for the emergent light beam

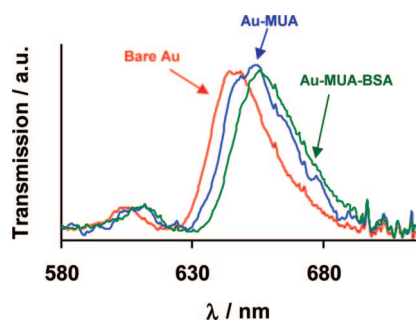


**FIGURE 2.** The effects of molecular adsorption on EOT.<sup>25</sup>

in contrast to the anisotropic distribution expected from simple diffraction. The beaming phenomenon is more pronounced when a single nanohole is surrounded by a grating structure.<sup>34</sup> In the case of arrays of nanoholes, each hole acts like a new point source. Therefore, collimated incident light is recovered as a still collimated output.

### 3. Exploring EOT for Surface Plasmon Resonance Sensing

The EOT through arrays of nanoholes depends on the optical properties of the metal–dielectric interfaces through eq 1. Therefore, the adsorption of molecules on the gold surface should shift the transmission peak wavelength, leading to a SP-mediated chemical sensor. Figure 2 shows a demonstration of the monolayer sensitivity of the SPR from arrays of nanoholes reported by our group.<sup>25</sup> The white light transmission spectrum through a clean array of nanoholes (bare Au surface) presents a distinct resonant peak. The gold surface was then modified by immersing the array of nanoholes in an ethanoic solution of mercaptoundecanoic acid (MUA), leading to a characteristic red shift in the wavelength of maximum transmission due to the changes in the dielectric properties of the surface, as predicted by eq 1. Further modification of the surface by a protein (bovine serum albumin, BSA) provoked an additional wavelength shift. The spectrum characteristic of a bare gold surface was recovered after the surface species were removed by a plasma cleaning treatment.<sup>25</sup>

The results presented in Figure 2 are reminiscent of the adsorption-induced shifts in the angle of minimum reflectivity in typical Kretschmann-configuration surface-plasmon resonance (SPR) experiments.<sup>11</sup> SPR is one of the most widely used tools for the study of binding in biochemical systems, and Figure 2 shows that similar results can be obtained using arrays of nanoholes.<sup>25</sup> In contrast to the commercial SPR sensors, the phase-matching condition for excitation of SPs in zero-order transmission is given by the periodicity of the holes (eq 1), and prism coupling is not required. This simplified optical setup is more suitable for miniaturization.

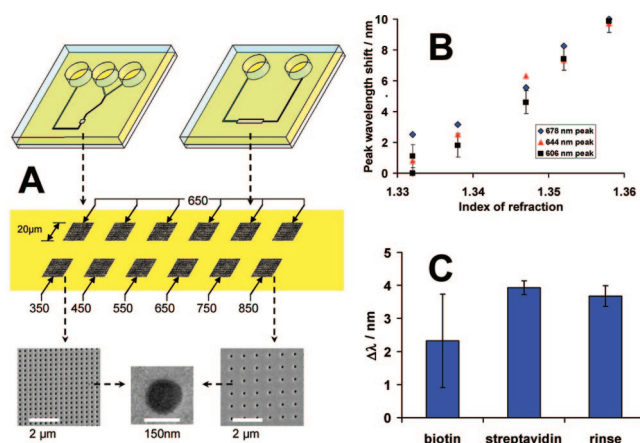


**FIGURE 3.** (A) Schematic and SEM images illustrating the architecture of the microfluidic chips with embedded nanohole arrays; (B) calibration curve using sucrose solutions with different concentrations; (C) application of nanoholes for an affinity test.<sup>26</sup>

The combination of all the interesting properties of SP-mediated transmission, including the highly localized sensing area and simple optical setup, render these types of substrates ideal for the development of integrated biosensors in laboratory-on-chip devices. This concept was demonstrated by our group,<sup>26</sup> and the devices investigated are shown in Figure 3A. Using standard microfluidics fabrication methods, we developed two configurations of the microfluidic layers, as shown in Figure 3A. The sensitivity of the integrated arrays of nanoholes was tested using standard sucrose solutions. The standard solutions were continuously flowed through the channels while the whole white light transmission spectra were measured in real time using the setup shown in Figure 1C. The calibration curve, presented in Figure 3B, yielded a linear trend within the range of refractive indexes investigated. The output sensitivity of each array was calculated from the slope of the calibration curves, averaging  $\sim 333$  nm/RIU (RIU = refractive index units).<sup>26</sup> The sensitivity found in our experiments agreed well with the values predicted for grating-based SPR devices<sup>35</sup> and are similar to the sensitivities obtained from sensing schemes based on metallic nanoparticles.<sup>36</sup>

The devices presented in Figure 3A were also used in affinity tests involving the biotin–streptavidin system.<sup>26</sup> Figure 3C summarized the results of the affinity tests performed using the arrays of nanoholes as sensor elements in the microfluidic device.

The results from Figure 3 demonstrate the potential of using arrays of nanoholes as sensing elements in laboratory-on-chip applications. The normal transmission setup allied to the small footprint of the arrays offers an attractive opportunity for miniaturization. An inexpensive device can be envisioned where the detection of the whole transmission

spectrum can be replaced by the measurements of changes in the amplitude of the transmission from a single laser source, a concept that has been reported already.<sup>37,38</sup>

The sensor output sensitivity obtained using the devices presented in Figure 3A is an order of magnitude smaller than the values from commercial angle-resolved SPR systems. This is not a fundamental limitation to the application of arrays of nanoholes for SPR sensing. It is important to point out that the sensing area of the arrays of nanoholes is much smaller than is typical of SPR arrangements; hence, the magnitude of the wavelength shift from our experiment originates from a smaller number of molecules. These considerations have been taken into account by Stark et al.,<sup>37</sup> who had demonstrated better sensitivity and resolution than commercial SPR devices by measuring the amplitude variations of a laser line through a short ordered nanohole array. SPR resolution on the order of commercial devices was also reported by Tetz et al.<sup>39</sup> In that case, they used crossed polarizers to select between the coherent and the incoherent contributions to the EOT (these are the contributions that lead to the Fano line shape observed in Figure 1B). This scheme allows the recovery of a symmetrical line shape for the transmission, which provides better sensitivity.<sup>39</sup>

#### 4. Nanohole-Enhanced Spectroscopy

The results from Figure 3 show the potential for the application of arrays of nanoholes in biomedical sensing and laboratory-on-chip devices. Since the SP fields are tightly confined to the interface, another powerful approach for chemical sensing is to take advantage of this localization to produce enhanced molecular spectroscopy. The EM localization is known as the main contribution to SERS and SEFS.<sup>14,15</sup> The application of SERS and SEFS as a highly sensitive analytical tool has been described for both random and patterned substrates.<sup>14,40</sup> Nanoholes in noble metals are a promising platform for enhanced spectroscopy because they not only confine the EM field but also restrict the analyte to very small volumes. Moreover, in contrast to colloidal particles dispersed on glass, the hot spots responsible for the field enhancement are specifically organized by the nanofabrication of the grating.<sup>41</sup> SERS measurements from a probe molecule, oxazine 720, adsorbed on arrays of nanoholes in gold films were obtained by our group.<sup>42</sup> The experimental geometry (forward scattering) is presented in Figure 4A. The Raman scattering of oxazine 720 was enhanced through the EOT of the laser excitation. The relationship between the SERS responses and the periodicity of the arrays was investigated, and it is

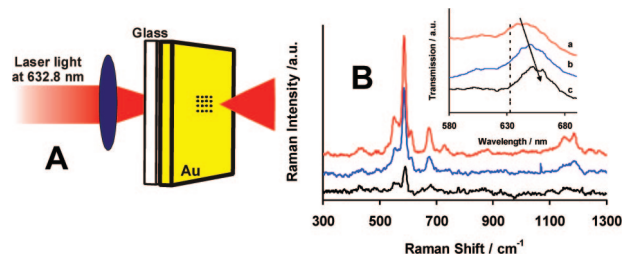


**FIGURE 4.** (A) Schematic of the forward scattering setup; (B) nanohole-enhanced Raman scattering from oxazine 720 from nanoholes with different periodicities ( $p$ ). The inset shows the transmission spectra of the arrays: (a)  $p = 560$  nm; (b)  $p = 590$  nm; (c)  $p = 620$  nm.<sup>42</sup>

shown in Figure 4B.<sup>42</sup> The inset in Figure 4B shows the transmission spectra of three arrays with different  $p$ -values. The dashed line corresponds to the laser excitation, fixed at 632.8 nm, and the arrow is to emphasize the position of the SP resonance relative to the laser line. It is clear that a strong enhancement is observed when the laser energy is closer to the SP excitation (red spectra), and the enhancement decreases as the separation between the laser energy and the EOT resonance increases.

The enhancement of the Raman signal was estimated to be of the order of  $10^5$  for oxazine 720 relative to the normal Raman of liquid benzene. This enhancement factor, however, includes resonance Raman (RR) contributions, since the laser excitation at 633 nm is within an electronic absorption of oxazine 720. Attempts to obtain SERS from other species, such as rhodamine 6G and pyridine, adsorbed on the nanoholes in gold were not successful, indicating that the additional RR contribution was essential for the observation of the spectra in Figure 4B. A quantitative evaluation of the enhancement factor from nanoholes in silver was realized by Reilly et al.<sup>43</sup> An enhancement factor of  $10^2$  due exclusively to the SP excitation through nanoholes was obtained. SERS from randomly distributed nanoholes in gold films and normal Raman from single nanoholes in metal were also reported.<sup>44,45</sup>

Infrared (IR) spectroscopy is another vibrational tool that provides complementary information to the Raman scattering. It has been shown that EOT through Ni meshes enhances the IR absorption from adsorbates.<sup>46</sup> A 2 orders of magnitude enhancement in the IR intensities was observed due to the increased interaction time provided by the trapped light at the interface in the form of SP waves.

Although vibrational spectroscopy (Raman and IR) offers unique spectral characteristics of a chemical species, several of the current biomedical assays utilize fluorescence probes. Therefore, there is a great interest in exploring the applicability of the arrays of nanoholes as substrates for SEFS,<sup>47–51</sup> aim-

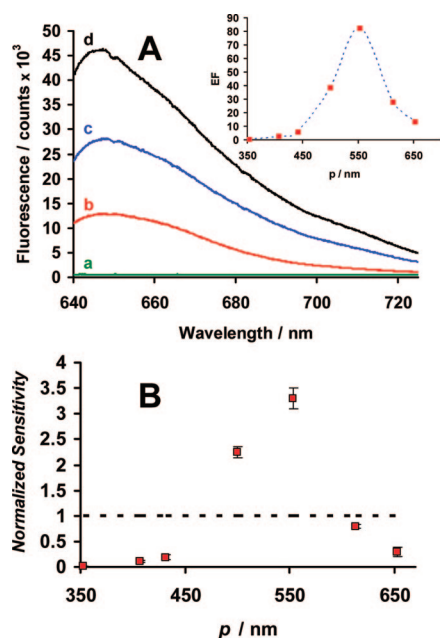


**FIGURE 5.** (A) Emission from arrays of nanoholes coated with a polystyrene film (PS) with (a)  $p = 553$  nm in the absence of the dye in the PS film (background), (b)  $p = 407$  nm and  $3 \mu\text{M}$  of dye embedded in the PS film, (c)  $p = 653$  nm and  $3 \mu\text{M}$  of dye embedded in the PS film, and (d)  $p = 553$  nm and  $3 \mu\text{M}$  of dye embedded in the PS film—the inset shows the calculated enhancement factor for all arrays investigated; (B) sensitivity obtained from plots of emission versus dye concentration in the PS film for arrays with different periodicities.<sup>47</sup>

ing at further improvement on the sensitivity and limit of detections of fluorescence-based biomedical tests.

The geometry of our SEFS experiments was similar to the one presented in Figure 4A, but now the nanoholes were covered with a polystyrene film doped with the dye.<sup>47</sup> The polystyrene is necessary because a film thicker than a monolayer is required for SEFS, due to the well-known fluorescence quenching experienced by emitters in close proximity to metallic surfaces. The fluorescence emissions from films of similar thickness but from arrays of nanoholes with different periodicities are shown in Figure 5A. The amount of fluorescence emissions from the arrays was always larger than expected from classical aperture theory when the conditions for SP resonance were achieved.

Another very relevant aspect for chemical analysis that was noted in our SEFS experiments<sup>47</sup> is illustrated in Figure 5B. The integrated fluorescence from each array was plotted against the concentration of dye in the film. The slope of these plots corresponds to the sensitivity from each array. The results from Figure 5B clearly show that the normalized sensitivity increased by more than three times when the conditions for EOT at the excitation laser frequency were achieved.<sup>47</sup> This is a very important observation because it

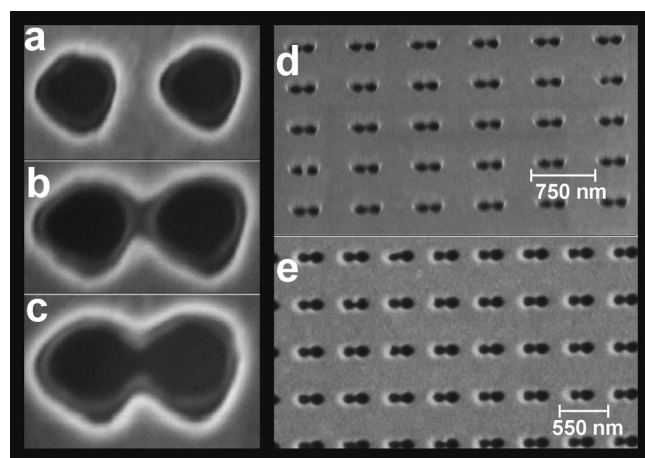


**FIGURE 6.** SEM picture of double holes ( $d$  is the center-to-center hole distance): (a)  $d = 250$  nm, hole diameter = 200 nm; (b)  $d = 210$  nm, hole diameter = 200 nm; (c)  $d = 190$  nm, hole diameter = 200 nm; (d) array of double holes with 750 nm periodicity; (e) arrays of double holes with 550 nm periodicity.<sup>54</sup>

demonstrates that not only the detection limit but also the optical response to concentration changes are optimized by the plasmonic structure.

## 5. Enhanced Spectroscopy and Sensing from Shaped Nanoholes

Another interesting feature that can be explored for chemical sensing and enhanced spectroscopy is the dependence of the EOT on the hole shape.<sup>7,33,52,53</sup> The anisotropic structures present selective polarization-dependent transmission. For instance, we had shown that elliptical holes act as nanopolarizers, with preferential transmission when the light field is polarized perpendicular to the major axis of the ellipse.<sup>52</sup> Similar effects have been observed for rectangular holes.<sup>53</sup> The line width of the transmission peak was also shown to depend on the aspect ratio of rectangular apertures;<sup>53</sup> therefore, structures with a sharper transmission band can be devised by geometric optimization to increase sensitivity.

One interesting hole shape that has been explored by our group for SERS and surface-enhanced second harmonic generation (SESHG) is the “double-hole” structure.<sup>33,54,55</sup> In this case, each single circular hole from a typical array is replaced by two holes separated by a controllable distance, as shown in Figure 6. The distance variation adds another degree of freedom for geometrical optimization of the plasmonic properties. An interesting situation arises when the two holes overlap. In this case, shown in Figure 6C, two sharp apexes are created. The apexes can act as an optical antenna, focusing the electromagnetic field to a very small region at the sharp

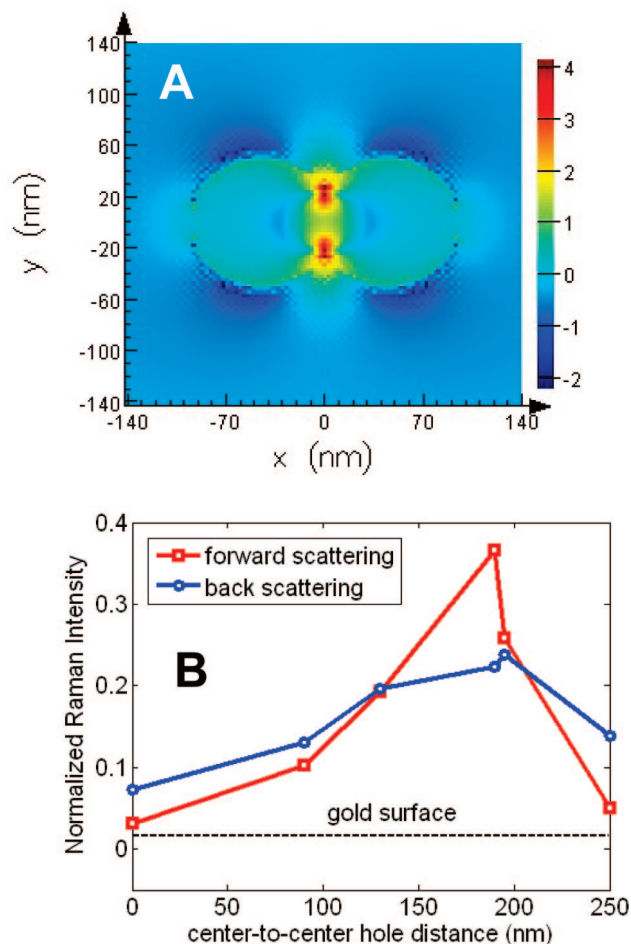


**FIGURE 7.** (A) FDTD calculation showing the enhanced field at the apexes of the double holes; (B) SERS as a function of the center-to-center hole distance within the double-hole basis. The array's periodicity was 750 nm, and the diameter of the nanoholes was 200 nm. The intensity of the  $591\text{ cm}^{-1}$  band of oxazine 720 was used.<sup>54</sup>

points at the apexes. Figure 7A shows a FDTD calculation of the field distribution around a double hole with overlapping holes.

It can be seen that the EM field is expected to be strongly concentrated in the apex regions. Since a strong localized field is the main requirement for enhanced spectroscopy, tunable surface enhancement is expected from these structures. We have obtained SERS from the double-hole structures with different hole distances. The dependence of the SERS efficiency versus the spacing between the holes in the basis of the lattice is shown in Figure 7B. It can be seen that, as expected from the electromagnetic theory, the SERS signal maximizes when the two holes overlap. The results from Figure 4 combined with the observations from Figure 7 show that the double-hole structure offers two degrees of freedom, shape and periodicity, for electric field optimization and enhanced spectroscopy. It is important to emphasize that the optimized cen-

ter-to-center hole offered an additional increase in the SERS that arises only from the molecules within the apex region. In other words, the number of species that are generating this extra enhancement is very small. Therefore, these antenna structures are promising for the detection of ultralow amounts of adsorbed species by SERS.

Beyond their application in enhanced spectroscopy, arrays of shaped nanoholes can also be optimized for SPR detection. Recently, it has been shown that the double-hole structures provide extra sensitivity to the response to refractive index changes.<sup>56</sup> Similar observations were obtained from the application of slits in gold films for SPR sensing.<sup>57</sup>

## 6. Outlook and Conclusions

In this Account, we described our contributions to the application of arrays of subwavelength holes in chemical sensing and enhanced spectroscopy. The arrays of nanoholes present significant advantages over other sensing schemes. They are ideal SPR sensors for a microfluidics environment, and their sensitivity may rival the performance of commercial SPR systems. The planar platform and transmission optics render this class of substrates ideal for multiplexing in microarray format. Microarrays, consisting of nanohole arrays as sensor elements, for multiple detection and high-throughput analysis seem to be the next step for this technology, and some preliminary examples have been proposed.<sup>38</sup>

In terms of applications in enhanced spectroscopy, arrays of circular nanoholes are suitable for SERS, SEFS, and SESHG. The enhancement factor obtained, however, is not as high as that observed from disordered structures. However, the enhancement properties of the arrays can be improved by using antenna structures. The double-hole structure, explored by our group, is a good example. In this case, it was shown that the geometry of the basis and the periodicity of the lattice can be independently optimized for maximum enhancement. The extra enhancement due to the antenna region originates only from the molecules adsorbed in the apexes. This indicates that this approach may be viable for the fabrication of structures for single-molecule SERS.

Looking more into future applications, it is noteworthy that nanoholes are unique among plasmonic nanostructures in that they are fundamentally channels. In sensor applications of nanohole arrays to date, these channels have been effectively dead-ended, and thus the transport between the sensor and the solution has been analogous to any other surface patterned sensor. While microfluidics has aided in delivering solutions to the arrays, the tremendous potential of the nano-

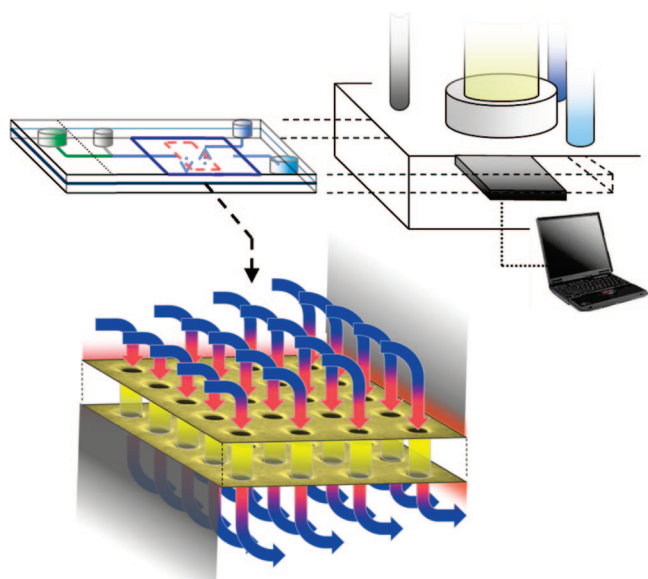


**FIGURE 8.** Schematic of flow-through nanohole array sensing as integrated in a chip-and-reader configuration. Flow to and through the nanohole/nanofluidic layer is facilitated by microfluidic service layers on top and bottom.

hole as a conduit has yet to be explored. We feel a flow-through nanohole array sensing format, as shown in Figure 8, presents several exciting possibilities: First, analyte transport via diffusion on the scale of the nanohole is extremely rapid, and thus flow-through greatly enhances the exposure of the active area to the solution under test. Likewise, a flow-through configuration could provide a model platform to study a range of dynamic processes; analogous electrochemical measurements in nanochannels that harness rapid diffusion on nanoscales show much promise.<sup>58</sup> Second, flow-through nanohole arrays, if connected in series with service microfluidics, would achieve a solution sieving action that is unique among surface-based sensing methods. Just as the nanophotonic structures enable intense confinement of the electromagnetic field, flow-through enables sieving and nanoconfinement of an adsorbed analyte in the same region. Third, while a single nanohole would present a dominant flow resistance in an otherwise microfluidic system, arrays serve to parallelize the resistance and thus fluid handling and control can be compatible between the parallel nanochannels and service microfluidics. Fourthly, flow-through provides access to a previously unexploited portion of the photonic structure and thus potentially new insight into EOT and new applications. One such application would be to immobilize a cell on the surface of a large array of nanoholes and use access provided by the through-nanoholes to deliver localized inputs and analyze localized outputs on the subcellular scale.

One of the glaring limitations to the wide ranging applicability of nanohole arrays in analytical chemistry is the serial

character of the FIB fabrication. However, several methods for large area patterning have been described in the literature.<sup>24,59</sup> These new lithographic methods offer a promising avenue to overcome this limitation.

*We gratefully acknowledge funding support for this work from NSERC, CFI, and BCKDF. We also thank current support through a NSERC SPG with the BC Cancer Agency and Micralyne Inc.*

#### BIOGRAPHICAL INFORMATION

**Reuven Gordon** is an Associate Professor in Electrical and Computer Engineering at the University of Victoria. His recent research contributions have been mainly in the area of nanophotonics.

**David Sinton** is an Assistant Professor in Mechanical Engineering at the University of Victoria. His research area is in micro- and nanofluidics.

**Karen L. Kavanagh** is a Physics Professor at Simon Fraser University. Her main fields of interest are electronic materials science and nanofabrication.

**Alexandre G. Brolo** is an Associate Professor of Chemistry at the University of Victoria. His current interests are on the development of substrates for enhanced spectroscopy and chemical sensing.

#### FOOTNOTES

\*To whom correspondence should be addressed. Phone: 1 250 721 7167. Fax: 1 250 721 7147. E-mail: agbrolo@uvic.ca.

#### REFERENCES

- Gates, B. D.; Xu, Q. B.; Stewart, M.; Ryan, D.; Willson, C. G.; Whitesides, G. M. New approaches to nanofabrication: Molding, printing, and other techniques. *Chem. Rev.* **2005**, *105*, 1171–1196.
- Willems, K. A.; Van Duyn, R. P. Localized surface plasmon resonance spectroscopy and sensing. *Annu. Rev. Phys. Chem.* **2007**, *58*, 267–297.
- Lal, S.; Link, S.; Halas, N. J. Nano-optics from sensing to waveguiding. *Nat. Photonics* **2007**, *1*, 641–648.
- Zhang, J. H.; Liu, H. Y.; Wang, Z. L.; Ming, N. B. Shape-selective synthesis of gold nanoparticles with controlled sizes, shapes, and plasmon resonances. *Adv. Funct. Mater.* **2007**, *17*, 3295–3303.
- Barnes, W. L.; Dereux, A.; Ebbesen, T. W. Surface plasmon subwavelength optics. *Nature* **2003**, *424*, 824–830.
- Zhao, J.; Zhang, X. Y.; Yonzon, C. R.; Haes, A. J.; Van Duyn, R. P. Localized surface plasmon resonance biosensors. *Nanomedicine* **2006**, *1*, 219–228.
- Degiron, A.; Ebbesen, T. W. The role of localized surface plasmon modes in the enhanced transmission of periodic subwavelength apertures. *J. Opt. A: Pure Appl. Opt.* **2005**, *7*, S90–S96.
- Ozby, E. Plasmonics: Merging photonics and electronics at nanoscale dimensions. *Science* **2006**, *311*, 189–193.
- Fang, N.; Lee, H.; Sun, C.; Zhang, X. Sub-diffraction-limited optical imaging with a silver superlens. *Science* **2005**, *308*, 534–537.
- Wei, X. Z.; Luo, X. G.; Dong, X. C.; Du, C. L. Localized surface plasmon nanolithography with ultrahigh resolution. *Opt. Express* **2007**, *15*, 14177–14183.
- Homola, J. Surface plasmon resonance sensor for detection of chemical and biological species. *Chem. Rev.* **2008**, *108*, 462–493.
- Rosi, N. L.; Mirkin, C. A. Nanostructures in biodiagnostics. *Chem. Rev.* **2005**, *105*, 1547–1562.
- Bangs, L. B. New developments in particle-based immunoassays: Introduction. *Pure Appl. Chem.* **1996**, *68*, 1873–1879.
- Aroca, R. *Surface-Enhanced Vibrational Spectroscopy*; Wiley: Chichester, U.K.; Hoboken, NJ, 2006.



- 15 Lakowicz, J. R. Plasmonics in biology and plasmon-controlled fluorescence. *Plasmonics* **2006**, *1*, 5–33.
- 16 Bethe, H. A. Theory of diffraction by small holes. *Phys. Rev.* **1944**, *66*, 163–182.
- 17 Wannemacher, R. Plasmon-supported transmission of light through nanometric holes in metallic thin films. *Opt. Commun.* **2001**, *195*, 107–118.
- 18 Gordon, R. Bethe's aperture theory for arrays. *Phys. Rev. A* **2007**, *76*, 053806.
- 19 Degiron, A.; Lezec, H. J.; Yamamoto, N.; Ebbesen, T. W. Optical transmission properties of a single subwavelength aperture in a real metal. *Opt. Commun.* **2004**, *239*, 61–66.
- 20 Ebbesen, T. W.; Lezec, H. J.; Ghaemi, H. F.; Thio, T.; Wolff, P. A. Extraordinary optical transmission through sub wavelength hole arrays. *Nature* **1998**, *391*, 667–669.
- 21 Genet, C.; Ebbesen, T. W. Light in tiny holes. *Nature* **2007**, *445*, 39–46.
- 22 Lezec, H. J.; Thio, T. Diffracted evanescent wave model for enhanced and suppressed optical transmission through subwavelength hole arrays. *Opt. Express* **2004**, *12*, 3629–3651.
- 23 Huang, C. P.; Wang, Q. J.; Zhu, Y. Y. Dual effect of surface plasmons in light transmission through perforated metal films. *Phys. Rev. B* **2007**, *75*, 245921.
- 24 Gao, H. W.; Henzie, J.; Odom, T. W. Direct evidence for surface plasmon-mediated enhanced light transmission through metallic nanohole arrays. *Nano Lett.* **2006**, *6*, 2104–2108.
- 25 Brolo, A. G.; Gordon, R.; Leathem, B.; Kavanagh, K. L. Surface plasmon sensor based on the enhanced light transmission through arrays of nanoholes in gold films. *Langmuir* **2004**, *20*, 4813–4815.
- 26 De Leebeek, A.; Kumar, L. K. S.; de Lange, V.; Sinton, D.; Gordon, R.; Brolo, A. G. On-chip surface-based detection with nanohole arrays. *Anal. Chem.* **2007**, *79*, 4094–4100.
- 27 Coe, J. V.; Heer, J. M.; Teeters-Kennedy, S.; Tian, H.; Rodriguez, K. R. Extraordinary transmission of metal films with arrays of subwavelength holes. *Annu. Rev. Phys. Chem.* **2008**, *59*, 179–202.
- 28 Genet, C.; van Exter, M. P.; Woerdman, J. P. Fano-type interpretation of red shifts and red tails in hole array transmission spectra. *Opt. Commun.* **2003**, *225*, 331–336.
- 29 Teeters-Kennedy, S.; Williams, S. M.; Rodriguez, K. R.; Cilwa, K.; Meleason, D.; Sudnitsyn, A.; Hrovat, F.; Coe, J. V. Extraordinary infrared transmission of a stack of two metal micromeshes. *J. Phys. Chem. C* **2007**, *111*, 124–130.
- 30 Rindzevicius, T.; Alaverdyan, Y.; Sepulveda, B.; Pakizeh, T.; Kall, M.; Hillenbrand, R.; Aizpurua, J.; de Abajo, F. J. G. Nanohole plasmons in optically thin gold films. *J. Phys. Chem. C* **2007**, *111*, 1207–1212.
- 31 Gordon, R.; Brolo, A. G. Increased cut-off wavelength for a subwavelength hole in a real metal. *Opt. Express* **2005**, *13*, 1933–1938.
- 32 van der Molen, K. L.; Klein Koerkamp, K. J.; Enoch, S.; Segerink, F. B.; van Hulst, N. F.; Kuipers, L. Role of shape and localized resonances in extraordinary transmission through periodic arrays of subwavelength holes: Experiment and theory. *Phys. Rev. B* **2005**, *72*, 045421.
- 33 Gordon, R.; Hughes, M.; Leathem, B.; Kavanagh, K. L.; Brolo, A. G. Basis and lattice polarization mechanisms for light transmission through nanohole arrays in a metal film. *Nano Lett.* **2005**, *5*, 1243–1246.
- 34 Lezec, H. J.; Degiron, A.; Devaux, E.; Linke, R. A.; Martin-Moreno, L.; Garcia-Vidal, F. J.; Ebbesen, T. W. Beaming light from a subwavelength aperture. *Science* **2002**, *297*, 820–822.
- 35 Moharam, M. G.; Gaylord, T. K. Rigorous Coupled-Wave Analysis of Metallic Surface-Relief Gratings. *J. Opt. Soc. Am. A* **1986**, *3*, 1780–1787.
- 36 Sun, Y. G.; Xia, Y. N. Gold and silver nanoparticles: A class of chromophores with colors tunable in the range from 400 to 750 nm. *Analyst* **2003**, *128*, 686–691.
- 37 Stark, P. R. H.; Halleck, A. E.; Larson, D. N. Short order nanohole arrays in metals for highly sensitive probing of local indices of refraction as the basis for a highly multiplexed biosensor technology. *Methods* **2005**, *37*, 37–47.
- 38 Lesuffleur, A.; Im, H.; Lindquist, N. C.; Lim, K. S.; Oh, S. H. Laser-illuminated nanohole arrays for multiplex plasmonic microarray sensing. *Opt. Express* **2008**, *16*, 219–224.
- 39 Tetz, K. A.; Pang, L.; Fainman, Y. High-resolution surface plasmon resonance sensor based on linewidth-optimized nanohole array transmittance. *Opt. Lett.* **2006**, *31*, 1528–1530.
- 40 Andrew, P.; Barnes, W. L. Molecular fluorescence above metallic gratings. *Phys. Rev. B* **2001**, *64*, 125405.
- 41 Krishnan, A.; Thio, T.; Kim, T. J.; Lezec, H. J.; Ebbesen, T. W.; Wolff, P. A.; Pendry, J.; Martin-Moreno, L.; Garcia-Vidal, F. J. Evanescently coupled resonances in SP enhanced transmission. *Opt. Commun.* **2001**, *200*, 1–7.
- 42 Brolo, A. G.; Arctander, E.; Gordon, R.; Leathem, B.; Kavanagh, K. L. Nanohole-enhanced Raman scattering. *Nano Lett.* **2004**, *4*, 2015–2018.
- 43 Reilly, T. H.; Chang, S. H.; Corbman, J. D.; Schatz, G. C.; Rowlen, K. L. Quantitative evaluation of plasmon enhanced Raman scattering from nanoaperture arrays. *J. Phys. Chem. C* **2007**, *111*, 1689–1694.
- 44 Bahns, J. T.; Yan, F. N.; Qiu, D. L.; Wang, R.; Chen, L. H. Hole-enhanced Raman scattering. *Appl. Spectrosc.* **2006**, *60*, 989–993.
- 45 Wenger, J.; Dintinger, J.; Bonod, N.; Popov, E.; Lenne, P. F.; Ebbesen, T. W.; Rigneault, H. Raman scattering and fluorescence emission in a single nanoaperture: Optimizing the local intensity enhancement. *Opt. Commun.* **2006**, *267*, 224–228.
- 46 Coe, J. V.; Rodriguez, K. R.; Teeters-Kennedy, S.; Cilwa, K.; Heer, J.; Tian, H.; Williams, S. M. Metal films with Arrays of tiny holes: Spectroscopy with infrared plasmonic scaffolding. *J. Phys. Chem. C* **2007**, *111*, 17459–17472.
- 47 Brolo, A. G.; Kwok, S. C.; Moffitt, M. G.; Gordon, R.; Riordon, J.; Kavanagh, K. L. Enhanced fluorescence from arrays of nanoholes in a gold film. *J. Am. Chem. Soc.* **2005**, *127*, 14936–14941.
- 48 Stark, P. R. H.; Halleck, A. E.; Larson, D. N. Breaking the diffraction barrier outside of the optical near-field with bright, collimated light from nanometric apertures. *Proc. Natl. Acad. Sci. U.S.A.* **2007**, *104*, 18902–18906.
- 49 Brolo, A. G.; Kwok, S. C.; Cooper, M. D.; Moffitt, M. G.; Wang, C. W.; Gordon, R.; Riordon, J.; Kavanagh, K. L. Surface plasmon-quantum dot coupling from arrays of nanoholes. *J. Phys. Chem. B* **2006**, *110*, 8307–8313.
- 50 Liu, Y.; Bishop, J.; Williams, L.; Blair, S.; Herron, J. Biosensing based upon molecular confinement in metallic nanocavity arrays. *Nanotechnology* **2004**, *15*, 1368–1374.
- 51 Blair, S.; Chen, Y. Resonant-enhanced evanescent-wave fluorescence biosensing with cylindrical optical cavities. *Appl. Opt.* **2001**, *40*, 570–582.
- 52 Gordon, R.; Brolo, A. G.; McKinnon, A.; Rajora, A.; Leathem, B.; Kavanagh, K. L. Strong polarization in the optical transmission through elliptical nanohole arrays. *Phys. Rev. Lett.* **2004**, *92*, 037401.
- 53 Koerkamp, K. J. K.; Enoch, S.; Segerink, F. B.; Hulst, N. F. v.; Kuipers, L. Strong influence of hole shape on extraordinary transmission through periodic arrays of nanoholes. *Phys. Rev. Lett.* **2004**, *92*, 183901.
- 54 Lesuffleur, A.; Kumar, L. K. S.; Brolo, A. G.; Kavanagh, K. L.; Gordon, R. Apex-enhanced Raman spectroscopy using double-hole arrays in a gold film. *J. Phys. Chem. C* **2007**, *111*, 2347–2350.
- 55 Lesuffleur, A.; Kumar, L. K. S.; Gordon, R. Apex-enhanced second-harmonic generation by using double-hole arrays in a gold film. *Phys. Rev. B* **2007**, *75*, 045423.
- 56 Lesuffleur, A.; Im, H.; Lindquist, N. C.; Oh, S. H. Periodic nanohole arrays with shape-enhanced plasmon resonance as real-time biosensors. *Appl. Phys. Lett.* **2007**, *90*, 261104.
- 57 Lee, K. L.; Lee, C. W.; Wang, W. S.; Wei, P. K. Sensitive biosensor array using surface plasmon resonance on metallic nanoslits. *J. Biomed. Opt.* **2007**, *12*, 044023.
- 58 Zevenbergen, M. A. G.; Krapf, D.; Zuidam, M. R.; Lemay, S. G. Mesoscopic concentration fluctuations in a fluidic nanocavity detected by redox cycling. *Nano Lett.* **2007**, *7*, 384–388.
- 59 Lim, C. S.; Hong, M. H.; Lin, Y.; Xie, Q.; Luk'yanchuk, B. S.; Kumar, A. S.; Rahman, M. Microlens array fabrication by laser interference lithography for super-resolution surface nanopatterning. *Appl. Phys. Lett.* **2006**, *89*, 191125.